

CRAMER-RAO BOUND ANALYSIS OF DISTRIBUTED DOA ESTIMATION EXPLOITING MIXED-PRECISION COVARIANCE MATRIX

Md. Waqeeb T. S. Chowdhury and Yimin D. Zhang

Department of Electrical and Computer Engineering, Temple University, Philadelphia, PA 19122, USA

ABSTRACT

In this paper, we analyze the Cramer-Rao bound of the distributed direction-of-arrival (DOA) estimation problem where the covariance matrix is formulated in a mixed-precision manner. In this scheme, the self-covariance matrix of a subarray is locally computed using the full-precision data received at the subarray, whereas one-bit data are exploited at the fusion center to compute the cross-covariance matrices between different subarrays. As such, the resulting covariance matrix of the distributed array consists of full-precision subarray self-covariance matrices and low-precision cross-covariance matrices between subarrays, thus termed as a mixed-precision covariance matrix. Such distributed DOA estimation scheme offers substantial reduction of the network communication overhead while maintaining the degrees of freedom offered by the distributed array. We provide the Cramer-Rao bound analysis which enables us to understand the importance of the self- and cross-covariance matrices and optimize the array parameters. The CRB analysis results are compared with the root mean-square error performance of the estimated signal DOAs.

Index Terms— Direction-of-arrival estimation, Cramer-Rao bound, mixed-precision covariance matrix, one-bit quantization, distributed array.

1. INTRODUCTION

Direction-of-arrival (DOA) estimation is an important technique in array signal processing [1, 2]. The recent development in, e.g., sensor networks and unmanned vehicles has promoted distributed and collaborative sensing to become an integral part of wireless sensing systems. When forming a large-scale array is infeasible or impractical, using distributed arrays, which are made up of multiple separately spaced array platforms with a small number of sensors, is an attractive option. In such platforms, fusing the information observed at multiple distributed subarrays forms a virtual array with a higher aperture, higher degrees of freedom (DOFs), and much more capable sensing capability [3–8].

Distributed array processing can be performed either coherently or noncoherently [3, 4]. In order to perform DOA estimation via coherent processing, the fusion center needs to receive data observed at all subarrays to compute the covariance matrix. This requirement demands a high volume of data traffic between the subarrays and the processing center. To mitigate this problem, a distributed DOA estimation scheme based on mixed-precision data is developed in [9]. In this scheme, each subarray computes the full-precision self-covariance matrix of the subarray and also the quantized one-bit data, which are sent to the fusion center. The fusion center computes the cross-covariance matrices between different subarrays using the one-bit data. As such, the resulting total covariance matrix of the distributed array consists of full-precision subarray self-covariance

matrices and low-precision cross-covariance matrices between subarrays, thus termed as a mixed-precision covariance matrix. Such distributed DOA estimation scheme offers substantial reduction of the network communication overhead while maintaining the high number of DOFs offered by the distributed array.

The objective of this paper is to provide an analysis of the Cramer-Rao bound (CRB) to understand the performance offered by the distributed DOA estimation approach exploiting a mixed-precision covariance matrix. The CRB analysis is considered to a general case where each subarray is a sparse linear array [10, 11]. By using coarray lags and lag interpolation, sparse arrays provide a much higher number of DOFs and improved robustness [12–19]. We focus on the analysis in the difference coarray-based DOA estimation problem, i.e., the number of sources is higher than the number of physical sensors. The derived CRB results are important to understand the offerings of the self- and cross-covariance matrices and to optimize the array parameters. The results are compared with the root mean-square error (RMSE) performance of the estimated signal DOAs.

Notations: We use lower-case (upper-case) bold characters to denote vectors (matrices). In particular, \mathbf{I}_N denotes the $N \times N$ identity matrix, and $\mathbf{0}$ denotes a vector or matrix of all zero elements with a proper dimension. $(\cdot)^*$, $(\cdot)^T$, and $(\cdot)^H$ respectively represent the conjugate, transpose, and Hermitian operations. Notation \otimes denotes the Kronecker product, $\text{vec}(\cdot)$ vectorizes a matrix, $\text{diag}(\cdot)$ and $\text{bdiag}(\cdot)$ form diagonal and block-diagonal matrices, and $\text{Tr}(\cdot)$ represents the trace operator. In addition, $[\mathbf{A}]_{u,v}$ denotes the (u, v) th element of matrix \mathbf{A} and $\mathbb{E}[\cdot]$ is the statistical expectation operator. $\mathcal{Q}(\cdot)$ denotes the element-wise one-bit quantization operation, $j = \sqrt{-1}$ stands for the unit imaginary number, and $\text{Re}(\cdot)$ and $\text{Im}(\cdot)$ respectively extract the real and imaginary parts of a complex entry. Moreover, the labels FP, MP and 1B denote full-precision, mixed-precision and one-bit data, respectively. Finally, $\mathbb{C}^{M \times N}$ denotes the $M \times N$ complex space.

2. SYSTEM MODEL

Consider a distributed array platform consisting of K collinear subarrays. The k th subarray consists of M_k sensors, which are located at $\mathbb{S}_k = \{p_{k,1}d, p_{k,2}d, \dots, p_{k,M_k}d\}$ for $k = 1, \dots, K$, where $d = \lambda/2$ and λ denotes the signal wavelength. It is assumed that all subarrays are fully synchronized and the subarray locations are precisely known. For convenience and without loss of generality, the sensor position $p_{k,m}d$ relative to its respective reference sensor position $p_{k,1}d$ is considered an integer multiple of d .

Consider L uncorrelated far-field narrowband signals impinging on the K subarrays from distinct angles $\boldsymbol{\theta} = [\theta_1, \dots, \theta_L]^T$. The baseband signal vector received at the k th subarray is expressed as:

$$\mathbf{x}_k(t) = \sum_{l=1}^L \mathbf{a}_k(\theta_l) s_l(t) + \mathbf{n}_k(t) = \mathbf{A}_k \mathbf{s}(t) + \mathbf{n}_k(t), \quad (1)$$

where $s_l(t)$ denotes the signal waveform impinging from direction θ_l , $\mathbf{s}(t) = [s_1(t), \dots, s_L(t)]^T$,

$$\mathbf{a}_k(\theta) = [e^{-jP_{k,1}\pi \sin(\theta)}, e^{-jP_{k,2}\pi \sin(\theta)}, \dots, e^{-jP_{k,M_k}\pi \sin(\theta)}]^T \quad (2)$$

is the steering vector of the k th subarray for a signal impinging from angle θ , and $\mathbf{n}_k(t)$ represents the additive circularly complex white Gaussian noise vector observed at the k th subarray with mean $\mathbf{0}$ and covariance matrix $\sigma_n^2 \mathbf{I}_{M_k}$. Matrix $\mathbf{A}_k = [\mathbf{a}_k(\theta_1), \mathbf{a}_k(\theta_2), \dots, \mathbf{a}_k(\theta_L)]$ is referred to as the manifold matrix of the k th subarray. We also define $\mathbf{A} = [\mathbf{A}_1^T, \mathbf{A}_2^T, \dots, \mathbf{A}_K^T]^T$ as the manifold matrix of the entire array for later use. The stacked received signal vector for all subarrays is denoted as

$$\mathbf{x}(t) = [\mathbf{x}_1^T(t), \dots, \mathbf{x}_K^T(t)]^T \in \mathbb{C}^{M \times 1}, \quad (3)$$

where $M = \sum_{k=1}^K M_k$ denotes the total number of sensors across all subarrays.

3. MIXED-PRECISION DOA ESTIMATION

3.1. Local Processing at Subarrays

The self-covariance matrix of the received data for the k th subarray is given as:

$$\mathbf{R}_k = \mathbb{E}[\mathbf{x}_k(t)\mathbf{x}_k^H(t)] = \mathbf{A}_k \mathbf{S} \mathbf{A}_k^H + \sigma_n^2 \mathbf{I}_{M_k}, \quad (4)$$

where $\mathbf{S} = \mathbb{E}[\mathbf{s}(t)\mathbf{s}^H(t)] = \text{diag}([\sigma_1^2, \sigma_2^2, \dots, \sigma_L^2])$ is the source covariance matrix with σ_l^2 , $l = 1, \dots, L$, denoting the power of the l th source.

In practice, the self-covariance matrix of the k th subarray is estimated using T available data samples, expressed as

$$\hat{\mathbf{R}}_k = \frac{1}{T} \sum_{t=1}^T \mathbf{x}_k(t)\mathbf{x}_k^H(t). \quad (5)$$

On the other hand, the k th subarray performs one-bit quantization of the received data and sends the results to the fusion center. The real and imaginary parts of signal vector $\mathbf{x}_k(t)$ are respectively quantized to form a one-bit signal vector, expressed as [20]:

$$\mathbf{y}_k(t) = \frac{1}{\sqrt{2}} \{ \mathcal{Q}[\text{Re}(\mathbf{x}_k(t))] + j \mathcal{Q}[\text{Im}(\mathbf{x}_k(t))] \}. \quad (6)$$

3.2. Centralized Processing at Fusion Center

When the full-precision data are available at the fusion center, it would compute the cross-covariance matrix between the received data at the k_1 th and k_2 th subarrays as:

$$\begin{aligned} \mathbf{R}_{k_1 k_2} &= \mathbb{E}[\mathbf{x}_{k_1}(t)\mathbf{x}_{k_2}^H(t)] \\ &= \mathbf{A}_{k_1} \mathbf{S} \mathbf{A}_{k_2}^H = \sum_{l=1}^L \sigma_l^2 \mathbf{a}_{k_1}(\theta_l) \mathbf{a}_{k_2}^H(\theta_l), \end{aligned} \quad (7)$$

for $k_1, k_2 = 1, \dots, K$ with $k_1 \neq k_2$.

As we consider one-bit data samples transferred from each subarray to the fusion center, the fusion center estimates the cross-covariance matrix between the k_1 th and k_2 th subarrays based on the one-bit, i.e.,

$$\mathbf{R}_{k_1 k_2}^{1B} = \mathbb{E}[\mathbf{y}_{k_1}(t)\mathbf{y}_{k_2}^H(t)]. \quad (8)$$

Based on the relationship between the one-bit covariance matrix and the normalized covariance matrix described in [21, 22], we can find the following relationship:

$$\mathbf{R}_{k_1 k_2}^{1B} = \mathbf{A}_{k_1} \text{diag}(\bar{\mathbf{p}}) \mathbf{A}_{k_2}^H, \quad (9)$$

where $\bar{\mathbf{p}} = [\bar{\sigma}_1^2, \dots, \bar{\sigma}_L^2]^T$ denotes the normalized signal power of the L sources with $\bar{\sigma}_l^2 = \sigma_l^2 / (\sigma_n^2 + \sum_{k=1}^L \sigma_k^2)$. It is noted that, as only the cross-covariance matrices between different subarrays are considered, the $\mathbf{R}_{k_1 k_2}^{1B}$ term in (9) does not include noise power entries because of the zero covariances.

Based on the arcsine relationship between the one-bit covariances $\mathbf{R}_{k_1 k_2}^{1B}$ and the normalized full-precision covariances $\bar{\mathbf{R}}_{k_1 k_2}$ [21, 23], we obtain

$$\bar{\mathbf{R}}_{k_1 k_2} = \sin\left(\frac{\pi}{2} \text{Re}[\mathbf{R}_{k_1 k_2}^{1B}]\right) + j \sin\left(\frac{\pi}{2} \text{Im}[\mathbf{R}_{k_1 k_2}^{1B}]\right). \quad (10)$$

Therefore, the cross-covariance matrix $\mathbf{R}_{k_1 k_2}$ between subarrays k_1 and k_2 accounting for the signal powers is obtained from $\bar{\mathbf{R}}_{k_1 k_2}^{1B}$ as [9]

$$\mathbf{R}_{k_1 k_2} = \mathbf{G}_{k_1}^{1/2} \bar{\mathbf{R}}_{k_1 k_2} \mathbf{G}_{k_2}^{1/2}, \quad (11)$$

where \mathbf{G}_k is a diagonal matrix with $[\mathbf{G}_k]_{m,m} = [\mathbf{R}_k]_{m,m}$ for $m = 1, \dots, M_k$.

4. CRB ANALYSIS

The unknown parameters in the underlying problem include the DOA and power of the L sources, respectively denoted as vectors $\boldsymbol{\theta} = [\theta_1, \dots, \theta_L]^T$ and $\mathbf{p} = [\sigma_1^2, \sigma_2^2, \dots, \sigma_L^2]^T$, and the noise power, denoted as σ_n^2 . Define $\boldsymbol{\omega} = [\omega_1, \dots, \omega_L]^T$ as the spatial frequencies of the L sources with $\omega_l = d \sin(\theta_l) / \lambda = \sin(\theta_l) / 2$. Then, the unknown parameters are grouped as an $(2L + 1) \times 1$ vector $\boldsymbol{\psi} = [\boldsymbol{\omega}^T, \mathbf{p}^T, \sigma_n^2]^T$.

We consider the stochastic CRB under the assumption that the sources are known to be uncorrelated [10, 24]. Using the pessimistic model developed in [22] and the arcsine relationship described in Section 3.2, we describe the probability model of $\mathbf{x}(t)$ in a compact form as $\mathbf{x}(t) \sim \mathcal{CN}(\mathbf{0}, \mathbf{R})$ with

$$\mathbf{R} = \begin{bmatrix} \mathbf{R}_1 & \mathbf{R}_{1,2} & \cdots & \mathbf{R}_{1,K} \\ \mathbf{R}_{2,1} & \mathbf{R}_2 & \cdots & \mathbf{R}_{2,3} \\ \vdots & \vdots & \ddots & \vdots \\ \mathbf{R}_{K,1} & \mathbf{R}_{K,2} & \cdots & \mathbf{R}_K \end{bmatrix}. \quad (12)$$

In this expression, \mathbf{R}_k represents the self-subarray covariance matrix for the k th subarray as defined in (4), whereas \mathbf{R}_{k_1, k_2} is the cross-subarray covariance matrix between the k_1 th and the k_2 th subarrays as defined in (11), where $k, k_1, k_2 = 1, \dots, K$.

The general expression of the Fisher information matrix (FIM) is given by

$$[\mathbf{F}]_{u,v} = -\mathbb{E} \left[\frac{\partial^2 \ln p(\mathbf{x}|\boldsymbol{\psi})}{\partial \psi_u \partial \psi_v} \right], \quad (13)$$

where ψ_u denotes the u th element of $\boldsymbol{\psi}$, such that $u, v \in \{1, 2, \dots, 2L + 1\}$.

Exploiting T snapshots, the (u, v) th element of the FIM corresponding to the covariance matrix \mathbf{R} is expressed as [10, 25, 26]:

$$\begin{aligned} \frac{1}{T} [\mathbf{F}]_{u,v} &= \text{Tr} \left(\mathbf{R}^{-1} \frac{\partial \mathbf{R}}{\partial \psi_u} \mathbf{R}^{-1} \frac{\partial \mathbf{R}}{\partial \psi_v} \right) \\ &= \left[(\mathbf{R}^T \otimes \mathbf{R})^{-\frac{1}{2}} \frac{\partial \mathbf{r}}{\partial \psi_u} \right]^H \left[(\mathbf{R}^T \otimes \mathbf{R})^{-\frac{1}{2}} \frac{\partial \mathbf{r}}{\partial \psi_v} \right]. \end{aligned} \quad (14)$$

Because we are interested in the CRB of the signal DOAs, we partition the parameter vector $\boldsymbol{\psi}$ as $\boldsymbol{\psi} = [\boldsymbol{\omega}^T \mid \mathbf{p}^T \sigma_n^2]^T$, and denote $\mathbf{r} = \text{vec}(\mathbf{R})$. Then, the FIM can be expressed as [10]

$$\frac{1}{T} \mathbf{F} = \begin{bmatrix} \boldsymbol{\Delta}_\omega \\ \boldsymbol{\Delta}_o \end{bmatrix}^H \begin{bmatrix} \boldsymbol{\Delta}_\omega & \boldsymbol{\Delta}_o \end{bmatrix} = \begin{bmatrix} \boldsymbol{\Delta}_\omega^H \boldsymbol{\Delta}_\omega & \boldsymbol{\Delta}_\omega^H \boldsymbol{\Delta}_o \\ \boldsymbol{\Delta}_o^H \boldsymbol{\Delta}_\omega & \boldsymbol{\Delta}_o^H \boldsymbol{\Delta}_o \end{bmatrix}, \quad (15)$$

where

$$\boldsymbol{\Delta}_\omega = \left(\mathbf{R}^T \otimes \mathbf{R} \right)^{-\frac{1}{2}} \begin{bmatrix} \frac{\partial \mathbf{r}}{\partial \omega_1}, \dots, \frac{\partial \mathbf{r}}{\partial \omega_L} \end{bmatrix}, \quad (16)$$

depends only on $\boldsymbol{\omega}$, whereas

$$\boldsymbol{\Delta}_o = \left(\mathbf{R}^T \otimes \mathbf{R} \right)^{-\frac{1}{2}} \begin{bmatrix} \frac{\partial \mathbf{r}}{\partial \sigma_1^2}, \dots, \frac{\partial \mathbf{r}}{\partial \sigma_L^2}, \frac{\partial \mathbf{r}}{\partial \sigma_n^2} \end{bmatrix} \quad (17)$$

depends on the other parameters.

Following the derivation in [10], if the FIM is invertible, the CRB of $\boldsymbol{\theta}$ can be expressed as the Schur complement of the $\boldsymbol{\Delta}_o^H \boldsymbol{\Delta}_o$ block as [27]:

$$\text{CRB}(\boldsymbol{\omega}) = \frac{1}{T} (\boldsymbol{\Delta}_\omega^H \boldsymbol{\Pi}_o^\perp \boldsymbol{\Delta}_\omega)^{-1}, \quad (18)$$

where $\boldsymbol{\Pi}_o^\perp = \mathbf{I} - \boldsymbol{\Delta}_o (\boldsymbol{\Delta}_o^H \boldsymbol{\Delta}_o)^{-1} \boldsymbol{\Delta}_o^H$. It is shown in [10] that the nonsingularity of FIM is equivalent to the nonsingularity of $\boldsymbol{\Delta}_o^H \boldsymbol{\Delta}_o$ and $\boldsymbol{\Delta}_\omega^H \boldsymbol{\Pi}_o^\perp \boldsymbol{\Delta}_\omega$.

In the following, we first review the results of the FIM using full-precision and one-bit data based on [10] and [22], and the FIM for the mixed-precision data is then derived.

4.1. FIM Using Full-Precision Data

Following the derivations in [10], we first define $\mathbf{a}_\mathbb{D}(\theta_l)$ as the steering vector of the coarray corresponding to the l th source and $\mathbf{J} \in \{0, 1\}^{M^2 \times (2D-1)}$ as a binary matrix such that $\mathbf{a}^*(\theta) \otimes \mathbf{a}(\theta) = \mathbf{J} \mathbf{a}_\mathbb{D}(\theta)$, where D denotes the cardinality of the set of non-negative virtual sensors of the difference coarray [19]. Denoting \mathbf{R}_{FP} as the covariance matrix obtained from the full-precision data, its vectorized form \mathbf{r}_{FP} is given as

$$\mathbf{r}_{\text{FP}} = \sum_{l=1}^L \sigma_l^2 \mathbf{J} \mathbf{a}_\mathbb{D}(\theta_l) + \sigma_n^2 \text{vec}(\mathbf{I}_M). \quad (19)$$

Its partial derivative with respect to the spatial frequency ω_l is obtained as

$$\frac{\partial \mathbf{r}_{\text{FP}}}{\partial \omega_l} = j2\pi \sigma_l^2 \cdot \mathbf{J} \cdot \text{diag}(\mathbb{D}) \cdot \mathbf{a}_\mathbb{D}(\theta_l), \quad (20)$$

and its partial derivatives with respect to the source power σ_l^2 and the noise power σ_n^2 are respectively given as

$$\frac{\partial \mathbf{r}_{\text{FP}}}{\partial \sigma_l^2} = \mathbf{J} \mathbf{a}_\mathbb{D}(\theta_l) \quad \text{and} \quad \frac{\partial \mathbf{r}_{\text{FP}}}{\partial \sigma_n^2} = \text{vec}(\mathbf{I}_M). \quad (21)$$

Substituting (20) and (21) into (15)–(18) renders the FIM and CRB.

4.2. FIM Using One-Bit Data

Now we formulate the FIM for the case when the covariance matrix of the entire array is computed from one-bit data [22]. Treating the multiple subarrays as a single sparse linear array, the full-precision normalized cross-covariance matrix $\bar{\mathbf{R}}_{\text{FP}}$ is given as

$$\bar{\mathbf{R}}_{\text{FP}} = \mathbf{A} \text{diag}(\bar{\mathbf{p}}) \mathbf{A}^H + \left(1 - \sum_{l=1}^L \bar{\sigma}_l^2 \right) \mathbf{I}_M. \quad (22)$$

From the arcsine law, we can obtain,

$$\mathbf{R}_{1\text{B}} = \frac{2}{\pi} \arcsine(\bar{\mathbf{R}}_{\text{FP}}). \quad (23)$$

Substituting (22) to (23) and vectorizing the result, we obtain

$$\mathbf{r}_{1\text{B}} = \frac{2}{\pi} \mathbf{J} \cdot \arcsine \left[\mathbf{A}^d \bar{\mathbf{p}} + \left(1 - \sum_{l=1}^L \bar{\sigma}_l^2 \right) \mathbf{e} \right], \quad (24)$$

where \mathbf{A}^d is the steering matrix corresponding to the difference coarray of the entire distributed array, and the column vector $\mathbf{e} \in \{0, 1\}^{(2D-1) \times 1}$ is defined such that $[\mathbf{e}]_i = \delta(i - D)$.

The partial derivative of $\mathbf{r}_{1\text{B}}$ with respect to spatial frequency ω_l can be formulated as

$$\frac{\partial \mathbf{r}_{1\text{B}}}{\partial \omega_l} = -4j \bar{\sigma}_l^2 \mathbf{J} \cdot \text{diag}(\mathbf{d}) \left[\text{diag}(\bar{\mathbf{h}}) \cdot \text{Re} \left(\mathbf{a}^d(\theta_l) \right) - \mathbf{e} + j \text{diag}(\mathbf{h}) \cdot \text{Im} \left(\mathbf{a}^d(\theta_l) \right) \right]. \quad (25)$$

Similarly, its partial derivatives with respect to the source power σ_l^2 and the noise power σ_n^2 are respectively given as

$$\frac{\partial \mathbf{r}_{1\text{B}}}{\partial \sigma_l^2} = \frac{2}{\pi} \mathbf{J} \left[\text{diag}(\mathbf{h}) \cdot \text{Re} \left(\mathbf{a}^d(\theta_l) \right) - \mathbf{e} + j \text{diag}(\bar{\mathbf{h}}) \cdot \text{Im} \left(\mathbf{a}^d(\theta_l) \right) \right] \quad (26)$$

and

$$\frac{\partial \mathbf{r}_{1\text{B}}}{\partial \sigma_n^2} = \frac{2}{\pi} \mathbf{J} \left[\text{diag}(\mathbf{h}) \cdot \mathbf{e} + j \text{diag}(\bar{\mathbf{h}}) \cdot \mathbf{e} \right], \quad (27)$$

where $\mathbf{d} = [-l_{D-1}d, \dots, 0, \dots, l_{D-1}d]^T$ denotes the locations of the virtual sensors of the difference coarray considering sensor locations of all subarrays combined. Also, \mathbf{h} and $\bar{\mathbf{h}}$ are given as

$$\mathbf{h} = \left[1 - \left| \text{Re} \left(\sum_{l=1}^L \bar{\sigma}_l^2 e^{j\mathbf{d}\pi \sin \theta_l} \right) \right|^2 \right]^{-1/2} \quad (28)$$

and

$$\bar{\mathbf{h}} = \left[1 - \left| \text{Im} \left(\sum_{l=1}^L \bar{\sigma}_l^2 e^{j\mathbf{d}\pi \sin \theta_l} \right) \right|^2 \right]^{-1/2}. \quad (29)$$

Similarly, substituting (25)–(27) into (15)–(18) renders the FIM and CRB. It is noted that, for the underlying case, because the one-bit data are used in computing (25)–(27), the one-bit covariance matrix $\mathbf{R}_{1\text{B}}$ is used in (16) and (17) in lieu of \mathbf{R} .

4.3. FIM Using Mixed-Precision Data

Denote a mask matrix $\boldsymbol{\Gamma} = \text{bdiag}(\mathbf{I}_{M_1}, \dots, \mathbf{I}_{M_K})$ such that $\boldsymbol{\Gamma} \circ \mathbf{R} = \boldsymbol{\Gamma} \circ \mathbf{R}_{\text{FP}}$ represents the block-diagonal self-covariance matrix entries in \mathbf{R} that are estimated using full-precision data, and denote $\bar{\boldsymbol{\Gamma}} = \mathbf{1} - \boldsymbol{\Gamma}$ such that $\bar{\boldsymbol{\Gamma}} \circ \mathbf{R} = \bar{\boldsymbol{\Gamma}} \circ \mathbf{R}_{1\text{B}}$ represents the off-block-diagonal cross-covariance matrix entries in \mathbf{R} that are estimated from one-bit data. Therefore,

$$\mathbf{R} = \boldsymbol{\Gamma} \circ \mathbf{R} + \bar{\boldsymbol{\Gamma}} \circ \mathbf{R} = \boldsymbol{\Gamma} \circ \mathbf{R}_{\text{FP}} + \bar{\boldsymbol{\Gamma}} \circ \mathbf{R}_{1\text{B}}. \quad (30)$$

Therefore, by using the partial derivatives of the covariance matrices respectively obtained for the full-precision and one-bit data in Sections 4.1 and 4.2, the FIM elements $\boldsymbol{\Delta}_\omega$ and $\boldsymbol{\Delta}_o$ exploited

in (16) and (17) can be computed based on the respective results corresponding to the full-precision and mixed-precision data. We denote the elements for the full-precision data as $\Delta_{\omega}^{\text{FP}}$ and $\Delta_{\sigma}^{\text{FP}}$ whereas those for the one-bit data as $\Delta_{\omega}^{\text{1B}}$ and $\Delta_{\sigma}^{\text{1B}}$. Further denoting $\Gamma_{\text{E}} = \text{diag}[\text{vec}(\Gamma)]$ and $\bar{\Gamma}_{\text{E}} = \text{diag}[\text{vec}(\bar{\Gamma})]$, the mixed precision FIM components can be computed as

$$\Delta_{\omega}^{\text{MP}} = \Gamma_{\text{E}} \Delta_{\omega}^{\text{FP}} + \bar{\Gamma}_{\text{E}} \Delta_{\omega}^{\text{1B}} \quad (31)$$

and

$$\Delta_{\sigma}^{\text{MP}} = \Gamma_{\text{E}} \Delta_{\sigma}^{\text{FP}} + \bar{\Gamma}_{\text{E}} \Delta_{\sigma}^{\text{1B}}. \quad (32)$$

Therefore, we can obtain the CRB of the sparse array for the mixed-precision data case from (18), (31) and (32). It is noted that, for the CRB to exist, the FIM must be nonsingular [10]. It can be inferred from the above expressions that the mixed-precision FIM is nonsingular and thus invertible when the full-precision and one-bit FIMs are nonsingular.

5. NUMERICAL RESULTS

We consider a distributed array consisting of two sparse subarrays. Each subarray consists of 3 sensors. $L = 7$ sources are assumed to arrive in $[-60^\circ, 40^\circ]$ with a uniform angular separation. The subarray configuration is given as

$$\mathbb{S}_1 = \{0, 1, 4\}d, \quad \mathbb{S}_2 = \{7, 9, 11\}d.$$

Fig. 1(a) shows the CRB and the RMSE performance of the distributed array with respect to the number of snapshots, K . When computing the RMSE results, the lag interpolation method described in [28] is used, and the results are computed from 100 independent trials. It is observed that, while inferior to the full-precision data case due to one-bit quantization in reconstructing the cross-covariances, with the only addition of the subarray self-covariance matrices, the mixed-precision processing offers a substantial improvement from the one-bit data case. Fig. 1(b) depicts the CRB and RMSE with respect to the input signal-to-noise ratio (SNR) of each signal and confirms a similar trend.

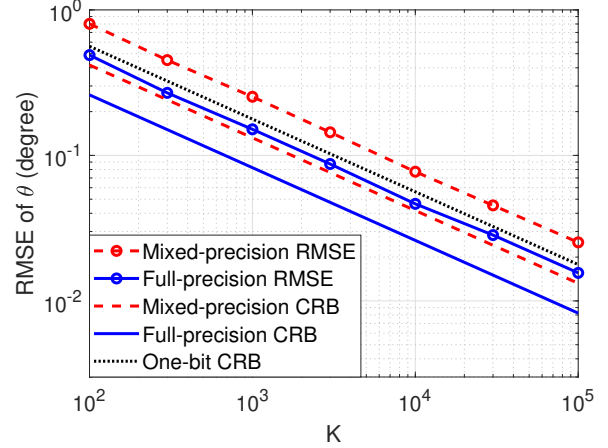
Fig. 2 shows the CRB with respect to the number of sources, L . Note that, as the number of interpolated array sensors is 12, the maximum number of sources that can be detected by the distributed array is 11. It is observed that the CRB degrades as the number of sources increases. Furthermore, the simulation results in both Figs. 1 and 2 confirm that the CRB corresponding to full-precision, mixed-precision, and one-bit data follow a similar trend irrespective of the parameters being considered.

6. CONCLUSION

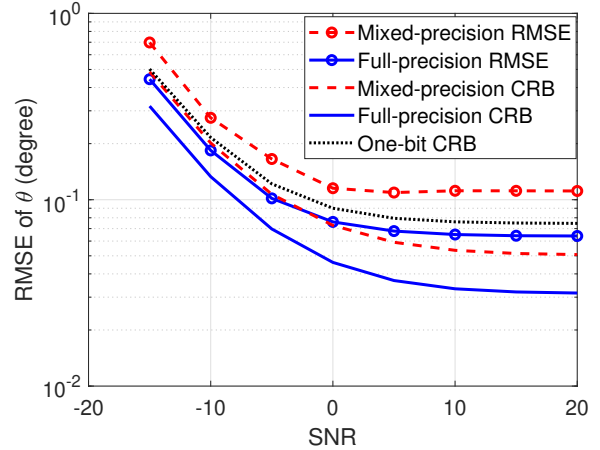
In this paper, we have analyzed the CRB for a distributed array exploiting mixed-precision covariance matrix. The analytical and simulation results confirmed the effectiveness of the distributed DOA estimation strategy using mixed-precision data that achieves a high estimation accuracy with significantly reduced network communication overhead. The results are also helpful for the design and optimization of distributed arrays.

7. ACKNOWLEDGEMENT

The authors are grateful to Dr. B. Shankar and Dr. S. Sedighi for their valuable suggestions.



(a) CRB and RMSE vs. number of snapshots (SNR = 5 dB)



(b) CRB and RMSE vs. SNR ($K = 5,000$ snapshots)

Fig. 1: Comparison of CRB and RMSE performance.

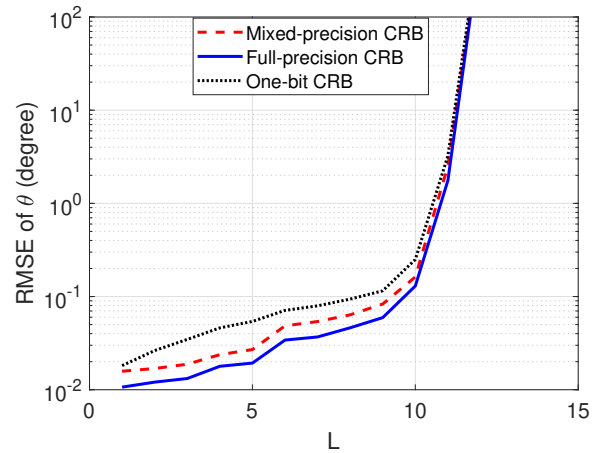


Fig. 2: CRB vs. number of sources (SNR = 5 dB, $K = 5,000$ snapshots)

8. REFERENCES

- [1] H. L. Van Trees, *Optimum Array Processing: Part IV of Detection, Estimation, and Modulation Theory*. Wiley, 2002.
- [2] E. Tuncer and B. Friedlander, *Classical and Modern Direction-of-Arrival Estimation*, Academic Press, 2009.
- [3] M. Pesavento, A. B. Gershman, and K. M. Wong, "Direction finding in partly calibrated sensor arrays composed of multiple subarrays," *IEEE Trans. Signal Process.*, vol. 50, no. 9, pp. 2103–2115, Sept. 2002.
- [4] W. Suleiman, P. Parvazi, M. Pesavento, and A. M. Zoubir, "Non-coherent direction-of-arrival estimation using partly calibrated arrays," *IEEE Trans. Signal Process.*, vol. 66, no. 21, pp. 5776–5788, Nov. 2018.
- [5] S. Zhang, A. Ahmed, and Y. D. Zhang, "Robust source localization exploiting collaborative UAV network," in *Proc. Asilomar Conf. Signals, Systems, and Computers*, Pacific Grove, CA, Nov. 2019.
- [6] P.-C. Chen and P. P. Vaidyanathan, "Distributed algorithms for array signal processing," *IEEE Trans. Signal Process.*, vol. 69, pp. 4607–4622, 2021.
- [7] M. W. T. S. Chowdhury and Y. D. Zhang, "Direction-of-arrival estimation exploiting distributed sparse arrays," in *Proc. Asilomar Conf. Signals, Systems, and Computers*, Pacific Grove, CA, Oct. 2021.
- [8] M. S. R. Pavel, M. W. T. S. Chowdhury, Y. D. Zhang, D. Shen, and G. Chen, "Machine learning-based direction-of-arrival estimation exploiting distributed sparse arrays," in *Proc. Asilomar Conf. Signals, Systems, and Computers*, Pacific Grove, CA, Oct. 2021.
- [9] Y. D. Zhang and A. Pratter-Bennette, "Collaborative direction-of-arrival estimation exploiting one-bit cross-correlations," in *Proc. Asilomar Conf. Signals, Systems, and Computers*, Pacific Grove, CA, Oct. 2021.
- [10] C.-L. Liu and P. P. Vaidyanathan, "Cramér-Rao bounds for coprime and other sparse arrays, which find more sources than sensors," *Digital Signal Process.*, vol. 61, pp. 43–61, 2017.
- [11] M. Guo, Y. D. Zhang, and T. Chen, "Performance analysis for uniform linear arrays exploiting two coprime frequencies," *IEEE Signal Process. Lett.*, vol. 25, no. 6, pp. 838–842, June 2018.
- [12] R. T. Hoctor and S. A. Kassam, "The unifying role of the coarray in aperture synthesis for coherent and incoherent imaging," *Proc. IEEE*, vol. 78, no. 4, pp. 735–752, April 1990.
- [13] P. P. Vaidyanathan and P. Pal, "Sparse sensing with co-prime samplers and arrays," *IEEE Trans. Signal Process.* vol. 59, no. 2, pp. 573–586, 2011.
- [14] S. Qin, Y. D. Zhang and M. G. Amin, "Generalized coprime array configurations for direction-of-arrival estimation," *IEEE Trans. Signal Process.*, vol. 63, no. 6, pp. 1377–1390, March, 2015.
- [15] H. Qiao and P. Pal, "Gridless line spectrum estimation and low rank Toeplitz matrix compression using structured samplers: A regularization-free approach," *IEEE Trans. Signal Process.*, vol. 65, no. 9, pp. 2221–2236, May 2017.
- [16] C. Zhou, Y. Gu, X. Fan, Z. Shi, G. Mao, and Y. D. Zhang, "Direction-of-arrival estimation for coprime array via virtual array interpolation," *IEEE Trans. Signal Process.*, vol. 66, no. 22, pp. 5956–5971, Nov. 2018.
- [17] Z. Zheng, W. Wang, Y. Kong and Y. D. Zhang, "MISC Array: A new sparse array design achieving increased degrees of freedom and reduced mutual coupling effect," *IEEE Trans. Signal Process.*, vol. 67, no. 7, pp. 1728–1741, April 2019.
- [18] S. Sun and Y. D. Zhang, "4D automotive radar sensing for autonomous vehicles: A sparsity-oriented approach," *IEEE Sel. Top. Signal Process.*, vol. 15, no. 4, pp. 879–891, June 2021.
- [19] A. Ahmed and Y. D. Zhang, "Generalized non-redundant sparse array designs," *IEEE Trans. Signal Process.*, vol. 69, pp. 4580–4594, 2021.
- [20] O. Bar-Shalom and A. J. Weiss, "DOA estimation using one-bit quantized measurements," *IEEE Trans. Aerosp. Electron. Syst.*, vol. 38, no. 3, pp. 868–884, July 2002.
- [21] J. H. Van Vleck and D. Middleton, "The spectrum of clipped noise," *Proc. IEEE*, vol. 54, no. 1, pp. 2–19, Jan. 1966.
- [22] S. Sedighi, M. R. B. Shankar, M. Soltanalian, and B. Ottersten, "On the performance of one-bit DoA estimation via sparse linear arrays," *IEEE Trans. Signal Process.*, vol. 69, pp. 6165–6182, 2021.
- [23] Y. Li, C. Tao, G. Seco-Granados, A. Mezghani, A. L. Swindlehurst, and L. Liu, "Channel estimation and performance analysis of one-bit massive MIMO systems," *IEEE Trans. Signal Process.*, vol. 65, no. 15, pp. 4075–4089, Aug. 2017.
- [24] M. Jansson, B. Goransson and B. Ottersten, "A subspace method for direction of arrival estimation of uncorrelated emitter signals," *IEEE Trans. Signal Process.*, vol. 47, no. 4, pp. 945–956, April 1999.
- [25] P. Stoica and A. Nehorai, "MUSIC, maximum likelihood, and Cramer-Rao bound," *IEEE Trans. Acoust., Speech, Signal Process.*, vol. 37, no. 5, pp. 720–741, May 1989.
- [26] P. Stoica, E. G. Larsson, and A. B. Gershman, "The stochastic CRB for array processing: A textbook derivation," *IEEE Signal Process. Lett.*, vol. 8, no. 5, pp. 148–150, May 2001.
- [27] A. Weiss and B. Friedlander, "On the Cramer-Rao bound for direction finding of correlated signals," *IEEE Trans. Signal Process.*, vol. 41, no. 1, pp. 495–499, Jan. 1993.
- [28] S. Liu, Z. Mao, Y. D. Zhang, and Y. Huang, "Rank minimization-based Toeplitz reconstruction for DoA estimation using coprime array," *IEEE Commun. Lett.*, vol. 25, no. 7, pp. 2265–2269, July 2021.